^{99m}Tc-ECD brain perfusion SPET: variability, asymmetry and effects of age and gender in healthy adults

Koenraad Van Laere[1], Jan Versijpt[1], Kurt Audenaert[2], Michel Koole[3], Ingeborg Goethals[1], Erik Achten[4], Rudi Dierckx[1]

[1] Division of Nuclear Medicine, P7, Ghent University Hospital, De Pintelaan 185, 9000 Ghent, Belgium
[2] Department of Psychiatry and Medical Psychology, Ghent University Hospital, Ghent, Belgium
[3] Medical Signal and Image Processing Department (MEDISIP), Ghent University, Ghent, Belgium
[4] Division of Neuroradiology, Radiology Department, Ghent University Hospital, Ghent, Belgium

Received 26 December 2000 and in revised form 5 April 2001 / Published online: 1 June 2001

Abstract. Reliable and high-resolution reference data for regional cerebral blood flow measured with single-photon emission tomography (SPET) are necessary for optimal clinical and research use. Therefore, a large dataset of normal technetium-99m labelled ethylene cysteine dimer (ECD) perfusion SPET in carefully screened healthy volunteers with an age range spanning six decades was created, with correction for non-uniform attenuation and scatter and based on an anatomically standardised analysis. Eighty-nine healthy volunteers, stratified for gender (46 females, 43 males; age 20–81 years), were included. Twelve volunteers underwent repeated ^{99m}Tc-ECD SPET after 2.5±2.3 weeks. An automated whole-brain volume of interest analysis with MANOVA as well as voxelwise analysis using SPM99 was conducted. Average intersubject variability was 4.8% while intrasubject reproducibility was 3.0%. An age-related decline in tracer uptake was found in the anterior cingulate gyrus, bilateral basal ganglia, left prefrontal, left lateral frontal and left superior temporal and insular cortex (all P=0.001–0.02). There was an overall increase in right/left asymmetry with age, which was most pronounced in the frontal and temporal neocortex. The most significant correlations between AI and age decade were found in the prefrontal (R=0.35, P=0.001) and superior temporal neocortex (R=0.43, P<0.001). Women had significantly higher uptake in the right parietal cortex (P<0.001), while men showed higher uptake in the cerebellum and the left anterior temporal and orbitofrontal cortex (all P<0.01). This normative dataset allows age- and gender-specific patient and group assessment of ^{99m}Tc-ECD perfusion SPET under a wide variety of clinical circumstances in relation to normal variations and highlights the importance of both age- and gender-specific normal datasets for optimal analysis sensitivity.

Keywords: Cerebral blood flow – ^{99m}Tc-ECD – Anatomical standardisation – Statistical parametric mapping – Normal aging

Eur J Nucl Med (2001) 28:873–887
DOI 10.1007/s002590100549

Koenraad Van Laere (✉)
Division of Nuclear Medicine, P7,
Ghent University Hospital, De Pintelaan 185,
9000 Ghent, Belgium
e-mail: koen.vanlaere@rug.ac.be
Tel.: +32-9-2403028, Fax: +32-9-2403807

Introduction

In the past few years, important advances have been made in both instrumentation and processing software for functional brain single-photon emission tomography (SPET). Improvements in resolution and sensitivity due to the use of fanbeam collimation allow the acquisition of technetium-99m labelled radioligands with a resolution of 7–8 mm full-width at half-maximum (FWHM). Correction for physical factors that degrade both image quality and the accuracy of quantification, such as attenuation and scatter, can now be performed on commercially available systems. Progress has also been made towards the automated analysis of functional imaging data involving retrospective intramodality registration to stereotactic templates as well as operator-independent intermodality co-registration to magnetic resonance imaging (MRI) or computed tomography (CT) data [1]. These techniques allow an automated predefined volume of interest (VOI) analysis [2] as well as voxel-based statistical testing [3], both of which have the advantage of objective and fast whole-brain perfusion analysis. This is in contrast to the prevailing clinical practice, where perfusion SPET scans of the brain are analysed in a qualitative fashion by visual inspection or by interactive region of interest (ROI) methods, both of which suffer from operator bias and are hence subjective. Automated, stan-

Table 1. Normal SPET data for brain perfusion (number of included subjects ≥ 20)

Ligand (99mTc labelled)	SPET camera: no. of heads, collimation*	Resolution, FWHM (mm)[a]	No. of subjects (M/F)	Age range (yrs)	Structural imaging	MR co-registration	Main findings	Reference	Comments
ECD	3, SHRFB	(8–9)	48 (22/26)	22–95	CT or MRI	No	Frontotemporal age gradient	[15]	Visual scoring and individually selected
							Asymmetry towards right hemisphere		
ECD	1, LEHR + 2 and 3, FB	8–15	28 (14/14)	57–81	MRI (4 subjects)	Partial	Asymmetry posterior and temporal	[14]	ROI analysis based on MR of 1 individual
									Low resolution
HMPAO	CERASPECT	7–8	152 (67/ 85)	50–92	CT or MRI	No	No global CBF changes with age	[35]	Only older age group
							↓ rCBF in ventricular regions		Singular value decomposition
							Higher rCBF for women in midcingulate, inferior parietal lobe bilaterally, inferior right temporal		Surface contour co-registration
HMPAO	1, LEHR	11	27 (17/10)	26–71	No	No	↓ L basal ganglia, frontal, occipital, L superior temporal, parietal	[19]	ROI analysis, 3 slices
							↑ Cingulate		Single-head low resolution
HMPAO	3, FB	(8–10)	44 (26/18)	20–73	CT or MRI	No	↓ Frontal most pronounced, also temporal and parietal	[34]	ROI analysis
					(>35 yrs)		Hockey stick model for age decline		
ECD	CERASPECT	7	33 (15/18)	4–15 and 27–56	CT	No	↓ Most cortical regions	[41]	Abnormal children
									Cerebellar normalisation
HMPAO	1, LEHR	16	68 (34/34)	19–45 and 65–79	CT	No	↓ L frontal and L posterior temporal	[21]	Low resolution
									No attenuation correction
HMPAO	3, LEHR	9.7	20 (11/9)	21–34 and 70–76	No	No	↓ Global neocortical	[20]	small group
							↑ Lateralisation towards R, mostly temporal		ROI analysis
HMPAO	3, FB	7.5	33 (20/13)	20 –76	No	No	↓ Frontal	[42]	ROI analysis CBF linearisation

Table 1. (continued)

Ligand (99mTc labelled)	SPET camera: no. of heads, collimation*	Resolution, FWHM (mm)[a]	No. of subjects (M/F)	Age range (yrs)	Structural imaging	MR co-registration	Main findings	Reference	Comments
HMPAO	3-slice Tomomatic	10	53 (27/26)	21–83	CT	Yes	↓ Frontotemporal	[43]	ROI analysis
							↑ Lateralisation towards R, mostly temporal		
^{133}Xe	–	>15	76 (38/38)	18–72	No	No	Absolute flow higher in women	[44]	Low resolution, 32 scintillation detectors
							rCBF in women higher in upper central, parietal and occipital regions		
							rCBF in women lower in left frontal region		

FB, Fanbeam; LEHR, low-energy high-resolution parallel beam

[a] Values in parentheses for resolution are not given in the article but have been estimated from other references concerning the same cameras

dardised and quantitative analysis would improve the diagnostic sensitivity of already approved and developing clinical applications of perfusion SPET imaging.

For optimal clinical and research use, techniques based on anatomical standardisation necessitate quantitative comparison with reliable and carefully selected normal data [4]. Normative datasets for perfusion SPET have been limited by small study samples, volunteer selection problems, limited age range, low-resolution equipment, the absence of scatter and/or attenuation correction, and absence of or limited structural matching (Table 1).

The tracers most widely used for SPET perfusion measurements, ^{99m}Tc-labelled ethylene cysteine dimer (ECD) and hexamethylpropyl amine oxime (HMPAO), are retained in the brain in a fixed distribution that reflects the cerebral perfusion pattern but have different uptake mechanisms. Since they differ in distribution in both healthy brain [5] and pathological states [6], both tracers have specific advantages depending on the clinical question. These differences in uptake also necessitate reliance on normal data for each individual radioligand. So far, most normative SPET studies have been conducted with ^{99m}Tc-HMPAO (Table 1). However, ^{99m}Tc-ECD has advantages – prolonged intrinsic in vitro stability, high cerebral retention, lower radiation burden, rapid blood clearance of metabolites and rapid elimination from extracerebral tissues – that make it of particular interest.

The aims of this prospective study were twofold. Firstly, we wished to create a large cross-sectional normative ^{99m}Tc-ECD regional cerebral blood flow (rCBF) dataset based on carefully screened healthy volunteers with an age range spanning six decades, with appropriate correction for scatter and non-uniform attenuation and using an anatomically standardised analysis. Secondly, we aimed to study in detail the co-variate effects of age, gender and handedness by means of (a) conventional multivariate statistics based on a VOI analysis with linear anatomical standardisation and (b) an optimised voxel-based statistical parametric mapping analysis (SPM99) with non-linear anatomical standardisation based on the individual's high-resolution MRI data.

Materials and methods

Subjects. The subjects for this study were recruited in response to advertisements in the University Hospital, in community newspapers and on the homepage of the nuclear medicine department. All included subjects underwent thorough medical screening, including a complete history and physical examination, blood and urine tests, full clinical neurological examination by a board-certified neurologist, and psychiatric examination and neuropsychological testing, both by a board-certified psychiatrist. All subjects underwent high-resolution MRI with T1 MPRAGE (magnetisation preparation rapid acquisition gradient-echo) and T2 sequences, the scans being examined by a board-certified neuroradiologist.

Table 2. Demographic and clinical data for the 89 volunteers

	Age group (yrs)						
	All	20–29	30–39	40–49	50–59	60–69	70–81
No.	89	24	14	15	16	10	10
Sex							
M	43	11	8	5	8	4	7
F	46	13	6	10	8	6	3
Age							
M	46.8 (18.3)	25.0	34.9	46.9	54.6	66.6	74.5
F	44.6 (16.9)	24.4	35.1	46.2	55.2	64.3	78.6
Education (no. of years)							
M	14.8 (3.2)	15.8	16.3	14.0	14.4	15.3	12.1
F	13.8 (2.9)	15.7	15.7	14.0	12.9	11.8	7.0
Blood pressure (mmHg)							
Systolic							
M	130 (11)	125	131	126	133	133	133
F	128 (15)	123	118	135	129	134	137
Diastolic							
M	84 (10)	81	85	83	88	90	79
F	82 (11)	78	77	83	88	89	77
Pulse (min^{-1})							
M	69 (9)	64	68	69	72	74	73
F	70 (7)	69	65	69	72	73	68
Height (cm)							
M	178 (7)	181	179	181	176	176	172
F	167 (6)	171	169	167	165	162	159
Weight (kg)							
M	80 (13)	77	84	86	78	82	75
F	66 (11)	65	67	64	67	69	61
MMSE	29.7 (0.6)	29.8	29.8	29.9	29.7	29.5	28.9
Handedness[a]							
R	80	19	14	14	14	9	10
Mixed	3	–	–	1	2	–	–
L	6	5	–	–	–	1	–

Values in parentheses indicate one standard deviation
MMSE, Mini-Mental State Examination (30-point scale)
[a] Reference [45]

Exclusion criteria based on history included: known disorders of the central nervous system (epilepsy, head trauma, structural abnormality on CT or MRI); previous unexplained unconsciousness; known psychiatric disease or first- or second-degree relative with hospitalisation for psychiatric disease, especially mood disorders or schizophrenia; known dementia of the Alzheimer or frontal lobe type in first- or second-degree relatives; presence of implanted electronic devices; substance abuse (alcohol, drugs or medication) or previous clinical treatment for complications of substance abuse; consumption of psychoactive medication during the past 3 months (antidepressants, hypnotics, sedatives etc.); diabetes mellitus; auto-immune diseases; and major internal heart, lung, liver or kidney disease. For ethical reasons and as a protective measure, subjects with possible pregnancy or a previous medical investigation with a radiation burden above 1 mSv during the past 6 months were also excluded.

Individuals with mild medical conditions such as controlled hypertension (P_{dia}/P_{syst} <95/140 mmHg), osteoporosis, mild obstructive/hyperreactive lung disease or minor problems with no known influence on brain perfusion were included in the study.

Blood screening tests included peripheral red and white blood cell count with differentiation, transaminases, creatinine, C-reactive protein, fasting glucose and total cholesterol. Possible clinically relevant disturbances were excluded.

The neuropsychological examination included a history interview as well as standardised tests to identify volunteers with evidence of behavioural, cognitive or memory impairment. Test procedures included a Dutch translation of the Mini-Mental State Examination (MMSE) [7], a Dutch version of the Stroop Colour Word Test [8], phonological and semantic verbal fluency (Controlled Oral Word Association Test) [9], parts of the Wechsler Memory Scale [10]) and the Trail Making Test [11]). Individuals with test scores that fell outside the normal range were excluded. The cut-off for the MMSE was set at 28 for individuals younger than 60 years and 27 for those above 60 years.

All SPET images were reviewed by an experienced nuclear medicine physician to exclude focal perfusion defects.

A total of 89 adults (46 women, 43 men; age range 20–81 years) were included. Each age group was stratified for gender. Demographic data for all subjects are summarised in Table 2. In total, six volunteers above 50 years (three women, three men) used antihypertensive medication (specific-acting beta-blockers, calcium channel blockers or ACE inhibitors). Their

blood pressure had been within the normal range, without any need for antihypertensive medication adjustment, for at least 6 months before the SPET study, and there was no MRI evidence of white matter lesions.

To assess intrasubject reproducibility, 12 volunteers (four men and eight women, average age 44.6±21.0 years) underwent repeated SPET scanning under identical conditions (mean scanning interval 2.5±2.3 weeks, range 1–7).

The study was approved by the local Ethics Committee of Ghent University Hospital. Written informed was obtained from all the volunteers prior to the MRI and SPET studies. These data form a central part of the so-called GO AHEAD project (Ghent Optimised Absolute High-Resolution ECD Adult Database).

Data acquisition. All subjects refrained from consumption of alcohol and caffeine during the 12 h prior to the study. All selected volunteers were injected with 925 MBq ^{99m}Tc-ECD (Dupont Pharmaceuticals Ltd., Brussels, Belgium) under resting conditions (eyes closed, low ambient noise level). SPET studies were performed on average 35 min [±12 (SD), range 28–72] post injection. All acquisitions were performed on a Toshiba GCA-9300A triple-headed camera (Dutoit Medical, Wijnegem, Belgium) equipped with high-resolution lead fanbeam collimators and transmission CT (TCT) sources. The measured tomographic resolution for ^{99m}Tc was 7.4 mm at the fixed radius of rotation of 132 mm.

Non-uniform attenuation correction was performed with ^{153}Gd or ^{99m}Tc TCT. ^{99m}Tc TCT was used for the chronologically first 14 patients for logistical reasons. We have demonstrated previously that there are no differences in brain quantification for these two transmission nuclides [12]. In the case of ^{99m}Tc, one rod was filled with 370 MBq (10 mCi) ^{99m}Tc solution, calibrated to the start of the first scan of up to six consecutive volunteers. For ^{153}Gd, three rod sources each containing 370 MBq were used. For transmission reconstruction, static blank scans were acquired with 200 kcounts per camera head for both radionuclides.

Acquisition was performed in continuous mode with 90 projections in a 128×128 matrix (pixel size 1.72 mm). The camera operated in segmented mode with double 120° rotation with 40 s per projection angle. Scatter windows were placed as described previously [12].

Data processing. Before scatter correction, fanbeam projections were converted to 128×128 parallel data in 4° bins by the floating-point rebinning software as supplied by the manufacturer (parallel pixel size 3.2 mm). A triple-energy window scatter correction was performed on the projection data (all windows filtered with a Butterworth filter of order 8, cut-off 0.16 cycles/pixel for the main and 0.09 cycles/pixel for the scatter windows) [12].

Non-uniform attenuation maps were calculated by means of a modified non-uniform Chang algorithm with 1 iteration, filtered back-projection and Butterworth filtering (order 8, cut-off 0.10 cycles/pixel). For ^{153}Gd, theoretical linear energy scaling coefficients were used to adjust the narrow-beam attenuation coefficients to 140 keV. Emission images were also reconstructed by filtered back-projection. A post-reconstruction Butterworth filter of order 8 and cut-off 0.13 cycles/pixel was applied.

The image datasets were automatically registered to an anatomically standardised (stereotactic) template with a voxel size and slice separation of 3.59 mm (64×64×64 matrix) (BRASS, Brain Registration and Automated SPET Semiquantification, Nuclear Diagnostics) [13]. A count difference cost function with an iterative downhill-simplex search algorithm was used for registration. On the template, 35 predefined VOIs were defined, with inclusion of all grey matter for semiquantification [2]. ^{99m}Tc-ECD uptake was adjusted to the whole brain VOI uptake. This VOI approach allows the acquisition of quantitative information on regional uptake values, intrasubject reproducibility, asymmetry indices and anteroposterior gradients.

Intrasubject reproducibility was defined as the average of the absolute value of the intra-individual differences for each region obtained from both scans. Uptake asymmetries were defined as % asymmetry = [(right-left)/(right+left)]×200. Anteroposterior gradients were calculated from the ratio of all frontal VOIs to both occipital VOIs.

Magnetic resonance imaging. MR images were obtained within 3 months of the first SPET scan in all subjects (mean difference =–1±3.5 weeks; range –11 to 7 weeks) with a 1.5 T Magnetom SP4000 scanner (Siemens, Erlangen, Germany). First, high-resolution anatomical imaging was performed with a 3D-MPRAGE {three-dimensional sequence [TR (ms)/TE (ms)/flip angle (degrees)/slices/slice thickness (mm)/matrix/FOV (mm)/NEX = 9.7/4/8/178/0.9/230×256/250/1]}, yielding T1-weighted sagittal images with a voxel size of 0.98×0.98×0.9 mm. Second, 5-mm-thick proton density-weighted and T2-weighted axial sections were acquired to screen for age-related cerebrovascular disease (TR/TE/matrix/NEX = 2170/20–80/192×256/1 – interslice gap 1 mm). The total scanning time was 15 min.

Statistical analysis. A multivariate analysis based on the general linear model was conducted with VOI regions as between-subject factors and age, gender and handedness as co-variates. Asymmetry analysis was derived from the same model, with age and gender as co-variates. For brain VOIs that showed significant age-related changes, non-linear trends were assessed by testing whether a quadratic regression equation significantly improved the proportion of variance accounted for by the model. Bonferroni correction was applied for multiple comparisons. Bivariate correlations between age and regional CBF were tested by the Pearson correlation test. All statistics were calculated with SPSS (v9.0 for Windows, SPSS Inc, Heverlee, Belgium).

SPM analysis. To additionally study co-variate effects based upon improved structural-based transformations, SPET images were also analysed after non-linear warping of the corresponding MR images using SPM99 (Wellcome Department of Cognitive Neurology, University College, London). Interfile data were translated to ANALYZE format by means of in-house software (MedCon). Calculations were performed with Matlab 5.3 (Mathworks Inc., Sherborn, Mass., USA). A subset of 81 optimally acquired 3D MPRAGE scans without motion artefacts were available for segmentation and co-registration for volunteers without a significantly different age or gender distribution from the full 89-volunteer dataset.

Non-linear anatomical standardisation to the stereotactic T1 template was performed with 12 affine parameters, 7×8×7 basis functions, 12 iterations and sinc 9×9×9 interpolation. For the study of age and gender effects, an affine anatomical standardisation was also assessed to cross-check possible effects related to non-linear warping. The resultant voxel size after anatomical standardisation was set at 3×3×3 mm. For statistical analysis, data were smoothed with a 12-mm 3D Gaussian kernel. The confounding effect of global activity was removed by proportional scaling to a global value of 50 ml/min per 100 g. A grey matter threshold of 0.40 was used.

Age-related differences were studied on a voxelwise basis in a correlation design. Linear as well as second-order polynomial voxelwise regression with the individual's age as the co-variate was investigated. To assess the magnitude of the non-linear effect

of age, the squared values were put in a study design as co-variates of interest and linear evolution of age as the co-variate of no interest. Gender and handedness differences were studied by comparing age-matched studies in a categorical population-comparison design with 1 scan/subject (voxelwise *t* test). Contrasts were defined to examine areas of higher tracer uptake in men versus women and vice versa. This SPM{Z} map was interrogated at the height threshold corresponding to P_{height}=0.001 and extent thresholds corresponding to P_{ext}<0.05 corrected for multiple comparisons, unless otherwise stated.

Results

Subject exclusion

In total, 18 subjects (20%) (mean age 57.8±11.9 years) were excluded for clinical reasons: two had a major depressive disorder, one had diabetes mellitus, seven had used forbidden medication (mainly hypnotics/tranquillisers), five had structural abnormalities (two frontal infarctions, one thalamic infarction, one frontotemporal meningioma and one case of leucoencephalopathy), one had a clear focal left parietal perfusion deficit on SPET, and two were healthy volunteers who withdrew from the study.

Clinical and demographic variables

The average education level was 14.8 years for men and 13.8 years for woman (Table 2). The MMSE score was negatively correlated with both age (R=–0.51, P<0.001) and education years (R=–0.34, P=0.001). There was a small but significant gender difference in body mass index (BMI=height/length^2) (25.2 for men and 23.6 for women, P=0.05).

rCBF distribution pattern and asymmetry

Figure 1 shows the normal ^{99m}Tc-ECD distribution for all bilaterally grouped VOIs, subdivided for male and female volunteers. The ^{99m}Tc-ECD uptake pattern is similar for all neocortical regions, with a relative increase towards the posterior cortex. The highest relative uptake with respect to the grey matter average is noted in the visual cortices, posterior cingulate, lentiform nuclei and cerebellar grey matter. Lower uptake, as seen in the smaller VOIs such as the orbitofrontal, anterior temporal, mesial temporal and pons regions, may be partly related to partial volume effects.

There was an overall tracer uptake asymmetry towards the right hemisphere (P<0.001), with an average asymmetry index (AI) of +1.4%. Significant regional asymmetries with respect to the overall effect were found in the orbitofrontal cortex (AI=8.2, P=0.0001), superior temporal gyrus (AI=5.7, P=0.004) and caudate head (AI=–2.9, P=0.003) (Bonferroni corrected, also corrected for age and gender) (Table 3).

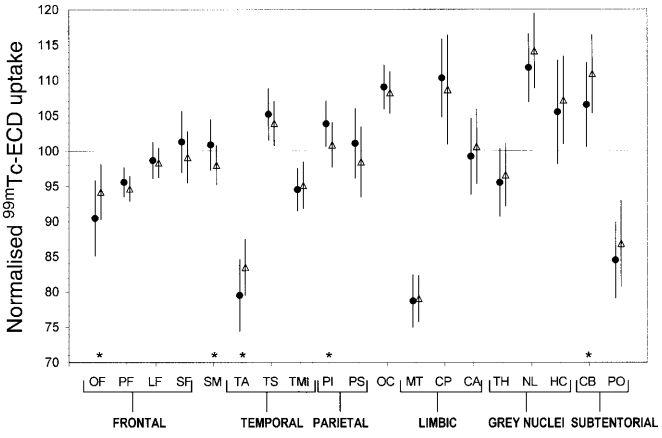

Fig. 1. Topography of normal ^{99m}Tc-ECD uptake, corrected for non-uniform attenuation and scatter, for both genders (*closed circles*, women; *open triangles*, men; significant differences are marked with an *asterisk* at the bottom of the figure). Data are normalised on total counts. The cortical regions are grouped by lobe in rostral to caudal order. This order heuristically reflects ontogenic and evolutionary development. *Error bars* represent one standard deviation. *OF*, Orbitofrontal; *PF*, prefrontal; *LF*, lateral frontal; *SF*, superior frontal; *SM*, sensorimotor; *TA*, temporal anterior; *TS*, temporal superior; *TMI*, temporal medial/inferior; *PI*, parietal inferior; *PS*, parietal superior; *OC*, occipital; *MT*, mesial temporal; *CP*, cingulate posterior; *CA*, cingulate anterior; *TH*, thalamus; *NL*, nucleus lentiformis; *HC*, head of caudate; *CB*, cerebellum; *PO*, pons

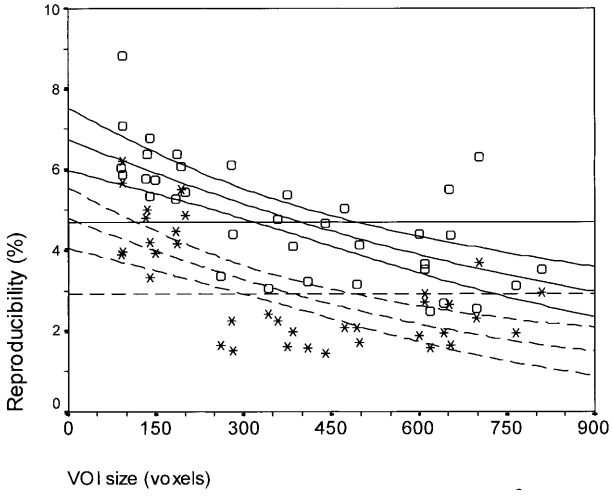

Fig. 2. Overall intersubject variability of ^{99m}Tc-ECD uptake of 89 healthy volunteers as a function of VOI size (*open symbols*). The intrasubject reproducibility for 12 subjects who underwent re-imaging is represented by the *asterisks*. *Horizontal lines* show the unweighted average variability (*solid line*, intersubject; *broken line*, intrasubject). The quadratic curve fits for the mean are also shown with 95% confidence limits

rCBF variability

The overall intersubject variability of ^{99m}Tc-ECD uptake is shown in Fig. 2 as a function of VOI size. The un-

Table 3. Asymmetry indices and correlation with age, both subdivided by gender. The asymmetry index is defined from the right and left ^{99m}Tc-ECD uptake values as (Right–Left)/(Right+Left) ×200. Significant deviations of the null hypothesis AI =0 are indicated. The asymmetry index correlated to age is given on the right side of the table

VOI[a]	AI[b]						Regression AI vs age					
	All	*P*	Men	*P*	Women	*P*	All, *R*	*P*	Men	*P*	Women	*P*
OF	8.2	0.0001**	8.4	0.002**	8.0	0.001**	0.24	0.025*	0.43	0.005**	0.07	NS
PF	0.2	NS	0.4	NS	0.0	NS	0.35	0.001**	0.55	0.0001**	0.25	NS
LF	1.3	NS	1.7	NS	0.9	NS	0.23	0.027*	0.28	(0.07)	0.23	NS
SF	2.0	NS	1.5	NS	2.4	NS	0.21	(0.052)	0.37	0.015*	0.07	NS
SM	2.4	NS	2.7	NS	2.3	NS	0.25	0.016*	0.17	NS	0.35	0.016*
TA	0.5	NS	–0.4	NS	1.4	NS	0.14	NS	0.12	NS	0.16	NS
TMI	0.0	NS	0.4	NS	–0.4	NS	0.20	(0.06)	0.08	NS	0.34	0.02*
TS	5.7	0.004**	5.8	(0.05)	5.7	0.03*	0.45	0.0001**	0.39	0.01**	0.53	0.0001**
PI	4.3	(0.05)	4.6	NS	4.1	NS	0.11	NS	0.01	NS	0.24	NS
PS	2.8	NS	2.4	NS	3.2	NS	–0.01	NS	0.09	NS	–0.09	NS
OC	5.0	0.02*	4.9	NS	5.1	NS	–0.02	NS	0.04	NS	0.02	NS
MT	0.9	NS	0.2	NS	1.7	NS	0.09	NS	0.09	NS	0.25	NS
TH	1.6	NS	2.4	NS	0.8	NS	–0.01	NS	0.14	NS	0.13	NS
NL	3.0	NS	2.0	NS	4.0	NS	–0.02	NS	–0.07	NS	0.02	NS
HC	–2.9	0.003**	–5.6	0.002**	–0.4	NS	0.18	(0.08)	0.16	NS	0.19	NS
CB	2.7	NS	2.1	NS	3.3	NS	0.04	NS	0.00	NS	0.08	NS

[a] Abbreviations for VOI regions are the same as in Fig. 1
[b] Values in parentheses denote AI or correlation significance of $0.05<P<0.10$
*$P<0.05$; **$P<0.01$

weighted average intersubject variability was 4.8%± 1.5% SD (range 2.5%–8.8%).

The intrasubject reproducibility for the 12 volunteers who underwent subsequent re-imaging is also shown in Fig. 2. The average intrasubject reproducibility was 3.0%±1.4% SD (range 1.4%–6.2%) and was significantly lower than the intersubject reproducibility ($P<0.001$). There was a negative correlation between VOI size (ξ), and intra- or intersubject uptake variability (σ) (R=–0.65, $P<0.001$). The relation was best modelled by a quadratic fit of the intersubject standard deviation to VOI size, given by $\sigma_{INTER}=6.7–0.0059\ \xi+1.8\ 10^{-6}\ \xi^2$ (R^2=0.48) and $\sigma_{INTRA}=4.8–0.0058\ \xi+2.3\ 10^{-6}\ \xi^2$ (R^2=0.57). This relationship also gives an estimation of the average variance for voxelwise analysis with these data when ξ approaches 1.

Age-related changes

Analysis of variance showed that both age and gender had a significant interaction effect with ^{99m}Tc-ECD VOI uptake ($P<0.001$). A decline with age was found for the anterior cingulate gyrus, bilateral basal ganglia, left prefrontal, left lateral frontal and left superior temporal and insular cortex (all P=0.001–0.02). Bilateral occipital activity increased significantly with age (P=0.001), as did the right inferior/medial temporal neocortex activity (P=0.002). Correlations between age and regional ^{99m}Tc-ECD uptake values are shown in Table 4. For the regions where significance was found, a non-linear (quadratic) age component was added to the analysis. Only in the case of the anterior cingulate was a significantly improved curve fit obtained, with an increased negative gradient after the age of 45–50.

The voxelwise regression design in SPM99 resulted in the same overall distribution, albeit with more regional detail. Figure 3 shows the results for the non-linear anatomical standardisation procedure and the age-related decreases. All significant cluster locations are given in Table 5. The contrast of increased tracer uptake with age merely showed significant clusters at the left and right cuneus in the occipital cortex.

The voxel-based linear regression model resulted in the same cluster locations and significance compared with a categorical two-population design (voxelwise t test) where the youngest three decades were contrasted with the oldest three decades.

In a regression model with both age and age^2 (age squared) as co-variates, there were no additional clusters showing a specific correlation with the quadratic component.

The results were slightly sensitive to the anatomical standardisation procedure. For the linear anatomical standardisation procedure, a more significant decrease with age was found in the anterior cingulate gyrus (T=6.31). Secondly, an additional cluster was present in the left temporo-parietal neocortex extending from the posterior part of the temporal superior gyrus to the inferior and superior parietal lobule (T=5.42), and, thirdly,

Table 4. Correlations between brain ^{99m}Tc-ECD uptake and age, normalised to total uptake, for both genders and for men and women separately. The last column indicates significant differences in correlation coefficient between men and women

VOI[a]		*R* all	*P*	Linear coeffic.	*R* men	*P*	Linear coeffic.	*R* women	*P*	Linear coeffic.	Δ linear coefficient M/F
OF	Left	0.10	NS	–0.37	0.03	NS	–0.07	0.19	NS	–0.81	NS
	Right	0.13	NS	0.36	0.43	0.003**	1.0	0.13	NS	–0.42	*
PF	Left	0.47	<0.001**	–0.65	0.58	<0.0001**	–0.72	0.37	0.006**	–0.57	NS
	Right	0.05	NS	–0.07	0.04	NS	–0.05	0.03	NS	–0.06	NS
LF	Left	0.50	<0.001**	–0.71	0.63	<0.0001**	–0.77	0.41	0.002**	–0.61	NS
	Right	0.06	NS	–0.14	0.13	NS	–0.22	0.05	NS	–0.01	NS
SF	Left	0.09	NS	–0.25	0.16	NS	–0.42	0.01	NS	–0.02	NS
	Right	0.10	NS	0.24	0.20	NS	0.36	0.07	NS	0.18	NS
SM	Left	0.14	NS	–0.24	0.15	NS	–0.23	0.10	NS	–0.17	NS
	Right	0.09	NS	0.27	0.01	NS	0.02	0.21	NS	0.64	NS
TA	Left	0.31	0.002**	–0.93	0.24	NS	–0.54	0.44	0.001**	–1.5	*
	Right	0.15	NS	–0.49	0.07	NS	–0.19	0.27	0.049*	–0.96	NS
TMI	Left	0.16	NS	0.29	0.14	NS	0.27	0.16	NS	0.27	NS
	Right	0.33	0.001**	0.83	0.20	NS	0.48	0.44	0.001**	1.2	NS
TS	Left	0.31	0.002**	–0.64	0.31	0.038*	–0.55	0.31	0.023*	–0.70	NS
	Right	0.17	(0.09)	0.47	0.12	NS	0.29	0.24	(0.08)	0.72	NS
PI	Left	0.14	NS	–0.23	0.22	NS	–0.36	0.01	NS	–0.02	NS
	Right	0.01	NS	0.04	0.15	NS	–0.35	0.21	NS	0.57	NS
PS	Left	0.02	NS	0.04	0.18	NS	–0.23	0.10	NS	0.34	NS
	Right	0.02	NS	–0.06	0.17	NS	–0.49	0.14	NS	0.45	NS
OC	Left	0.32	0.002**	0.68	0.40	0.007**	0.85	0.24	(0.08)	0.53	NS
	Right	0.35	<0.001**	0.66	0.43	0.003**	0.74	0.30	0.029*	0.62	NS
MT	Left	0.03	NS	–0.08	0.19	NS	0.42	0.23	NS	–0.62	NS
	Right	0.06	NS	0.19	0.15	NS	0.42	0.02	NS	–0.08	NS
TH	Left	0.12	NS	0.43	0.23	NS	0.67	0.02	NS	0.10	NS
	Right	0.16	NS	0.53	0.12	NS	0.43	0.27	NS	0.66	NS
NL	Left	0.30	0.002**	–1.1	0.31	0.04*	–1.1	0.32	0.02	–1.2	NS
	Right	0.32	0.001**	–1.3	0.34	0.023*	–1.2	0.37	0.006**	–1.4	NS
HC	Left	0.42	0.0001**	–2.1	0.41	0.005**	–2.1	0.42	0.002**	–2.2	NS
	Right	0.26	0.009**	–1.2	0.31	0.036*	–1.1	0.27	(0.05)	–1.3	NS
CB	Left	0.09	NS	0.36	0.16	NS	0.56	0.08	NS	0.03	NS
	Right	0.13	NS	0.46	0.21	NS	0.62	0.04	NS	0.15	NS
CA		0.53	<0.0001**	–1.6	0.53	<0.0001**	–1.5	0.56	<0.0001**	–1.8	NS
CP		0.02	NS	0.09	0.11	NS	–0.45	0.21⁄	NS	0.71	NS
PO		0.13	NS	0.43	0.21	NS	0.68	0.03	NS	0.09	NS

[a] Abbreviations for VOI regions are the same as in Fig. 1
*P<0.05; **P<0.01

there was a cluster at the right lateral frontal neocortex (T=4.58). For the activation contrast, affine anatomical standardisation resulted in two additional clusters located at the lateral sides of both thalami.

Concerning asymmetry, the overall VOI asymmetry index was weakly correlated with age (R=0.10, P<0.001) (Table 3). There was an overall increase in right/left asymmetry with age, which was most pronounced in the frontal and temporal neocortex. The most significant correlations between AI and age decade were found in the prefrontal (R=0.35, P=0.001) and superior temporal neocortex (R=0.43, P<0.001).

The anteroposterior gradient was significantly correlated with age (R=–0.39, P<0.001), with a gradient of –0.7%±0.2% SD per decade. However, if only data above the age of 40 were considered, no significant correlation remained.

As a function of age, there was a significant increase in mean intersubject standard deviation, ranging from 4.4 to 5.4 for the oldest decade (R=0.15, P=0.025).

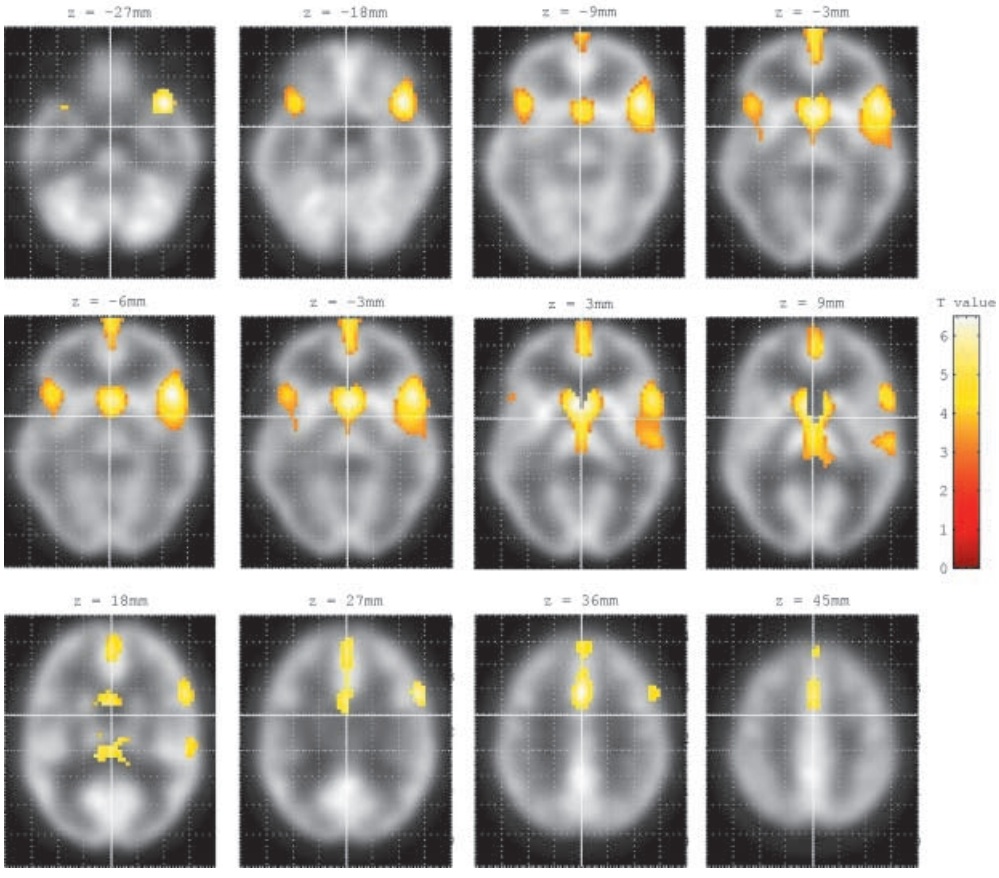

Fig. 3. Age dependence of ^{99m}Tc-ECD uptake. An SPM99 analysis with non-linear anatomical standardisation on the individual's MPRAGE T1 images was conducted with a linear regression design versus age. The glass brain projection images show voxels with a significant correlation with age at thresholds for cluster extent P_{ext}=0.001 and voxel intensity P_{height}=0.05 (corrected for multiple comparisons). These voxels are overlaid on a SPET template obtained from the volunteers participating in the study. Orientation is according to radiological convention

Gender differences

On the VOI analysis, women showed a significantly higher tracer uptake in the bilateral inferior and superior parietal cortex (mean difference in ^{99m}Tc-ECD uptake =3.3%±1.0%; P<0.001 after Bonferroni correction) (Fig. 4). These differences were also separately investigated for the young (20–50) and elderly (50–81) volunteers, and remained unchanged. On the other hand, men showed a significantly higher tracer uptake in the cerebellum, left anterior temporal cortex and orbitofrontal cortex (all P<0.01).

This was also shown by the categorical SPM analysis with non-linear warping in Fig. 5, albeit with two differences. The left parietal cluster was present only at the lower height threshold of P=0.05 (corrected) (women>men), while for the men>women contrast, an extension of the orbitofrontal cluster towards the anterior cingulate region was present on the voxel-based analysis. The exact cluster locations and their significance are given in Table 6.

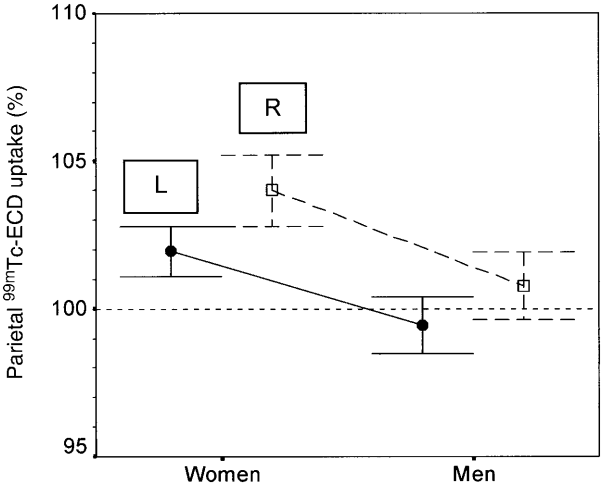

Fig. 4. Differences in ^{99m}Tc-ECD uptake between men and women as obtained by a VOI analysis for both parietal regions. The statistical threshold was set at P<0.01, corrected for multiple comparisons. The *error bars* indicate one standard deviation

Age by gender interaction

Significant differences for men and women in age-related tracer uptake changes were present in the right orbitofrontal VOI (P=0.003 for men, NS for women) and left anterior temporal pole (P=0.001 for women, NS for men) (Table 4). Separate linear SPM regression with age for the male and female populations showed that the right insular cortex reached significance for men but not

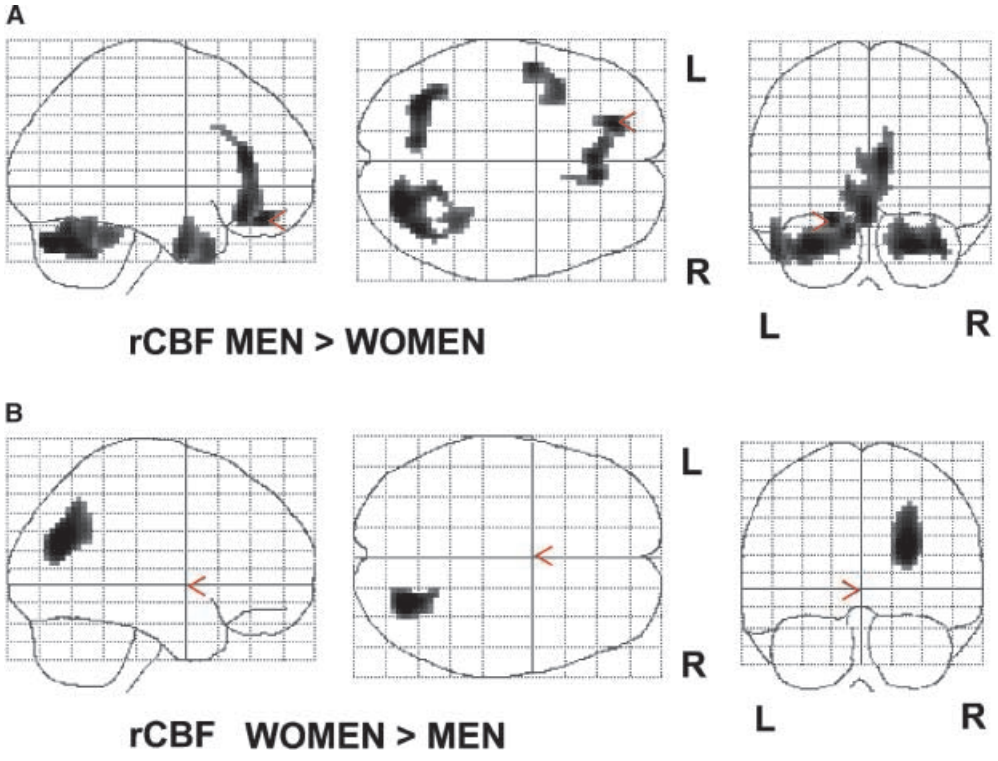

Fig. 5A, B. Differences in ^{99m}Tc-ECD tracer uptake between men and women. An SPM99 analysis of age-matched groups was conducted using anatomical standardisation with non-linear MPRAGE T1 warping of the subject's individual MRI. **A** The contrast "men<women" is shown, where significant voxels are presented on glass brain projections. **B** Here the contrast "men>women" is shown. In both figure parts, the thresholds were P_{ext}=0.01 for cluster extent and P_{height}=0.05 for voxel intensity (corrected for multiple comparisons)

Table 5. SPM analysis with age as co-variate. Significant clusters for increase and decrease in tracer uptake are given, corrected for multiple comparisons. Height threshold *P*=0.001, and extent threshold 50 voxels (*P*=0.05), corrected for multiple comparisons. Voxel size = 3×3×3 mm

Cluster level		Voxel level		Co-ordinates, maximal significant voxel	Region (Brodmann area)
P (corr.)	k_E	*P* (corr.)	*T*	*x,y,z* (mm)	
Decrease with age					
0.000	1,136	0.000	6.51	–45, 18, –12	L insula + gyrus frontalis inferior (BA 47)
		0.028	4.65	–54, 18, 18	L gyrus temporalis superior (BA 38)
0.000	1,159	0.000	6.26	3, 9, 3	Thalamus
		0.011	4.96	0, –9, 9	Head of caudate
		0.011	4.94	0, 18, 39	Cingulate (BA 32, 24) and mesial frontal (BA 9)
0.024	245	0.020	4.77	39, 18, –12	R insula + gyrus frontalis inferior (BA 47)
Increase with age					
0.001	163	0.000	5.61	–24, –105, 3	R occipital – cuneus (BA 18)
0.002	66	0.002	5.38	18, 105, 0	L occipital – cuneus (BA 18)

P, Probability; corr., corrected; k_E, cluster extent (voxels); *T*, SPM *t* statistic

for women at P_{height}=0.05. Similarly, uptake in the anterior cingulate cortex decreased significantly with age for women but not for men (down to P_{height}=0.05). Other clusters were the same as for both groups separately, and no additional clusters were found at the P_{height}=0.05 (corrected) level.

The evolution of asymmetry with age showed a marked difference between men and women in the frontal regions (Table 3). Highly significant frontal lateralisation takes place in aging men, while this is not the case for women. On the other hand, the change in asymmetry with age was greater for women in the superior temporal and sensorimotor cortex compared with men. Asymmetry in the caudate head reached significance only for men (lower on the left side), but no significant increase in asymmetry with age was observed.

For the anteroposterior gradient, there was no significant gender effect (*P*=0.49) or interaction between age and gender (*P*=0.34).

Concerning intersubject variability, there was no significant differential increase in variability between men and women for all VOIs (*P*=0.45).

Table 6. SPM analysis as a function of gender. Age was included as co-variate of no interest. Significant clusters for men > women and women > men (P_{height}=0.001, P_{ext}=0.05, corrected for multiple comparisons)

Cluster level		Voxel level		Co-ordinates, maximal significant voxel	Region (Brodmann area)
P (corrected)	k_E	*P* (corr.)	*T*	*x,y,z* (mm)	
Women >men					
0.013	255	0.03	4.76	24, –69, 28	R parietal + posterior gyrus temporalis medius (BA 39)
Men>women					
0.000	403	0.008	5.38	24, –78, –33	R cerebellum
0.000	202	0.033	5.00	–33, –83, –33	L cerebellum
0.000	281	0.037	4.87	21, 45, –18	Orbitofrontal (BA 11)
		0.043	4.81	–8, 33, 18	Anterior cingulate (BA 32)
0.001	495	0.019	4.95	–51, –3, –28	L anterior temporal – gyrus temporalis inferior (BA 21)

P, Probability; k_E, cluster extent (voxels); *T*, SPM *t* statistic

Handedness

Analysis of variance with asymmetry values as the dependent factor, adjusted for age and gender, VOI region as the within-subject factor and handedness as the co-variate, did not show a significant factor interaction between VOI region and handedness (*P*=0.44). In conjunction with these findings, when the six left-handed subjects were compared with 12 right-handed individuals, matched for age and gender, SPM analysis did not show any significant differences between perfusion scans with respect to handedness as high as at the P_{height}=0.05 level. Also, the full SPM modelling of all data with handedness score as the scaled co-variate did not reveal significant differences.

Discussion

Screening and inclusion criteria

The establishment of truly normal perfusion data requires careful screening and selection of healthy volunteers [4]. This issue has been addressed in very few previously published studies. With particular regard to ^{99m}Tc-ECD, no reference dataset based on such careful screening has been published. Our high percentage of excluded subjects after the rigid screening procedure is indicative of the recruitment difficulties when establishing reference data in healthy volunteers, but also of the possible pitfalls in functional studies that do not rely on high-resolution structural imaging. The rigid screening criteria make it unlikely that age-associated findings were confounded by brain disease, which may differentially affect the elderly. Because of the reliance on a cross-sectional design, we were not able to control for the influence of cohort effects and secular trends. Age was negatively correlated with education; furthermore, gender differences with respect to education were present at ages above 50 years, with females being less highly educated, a characteristic of the social situation in the mid-twentieth century. A relationship between education, not confounded by age, and volumetric or functional brain imaging parameters is still controversial and would require further study.

Confounding factors such as non-neurological medical history (hypertension, cardiac disease etc.) and medication were not fully evaluated. A medication effect would seem most likely in those individuals receiving antihypertensive medication. This study included only six volunteers (three male and three female) receiving such medication; none showed structural cerebral effects due to possible long-standing hypertension before the diagnosis was made. A separate SPM analysis did not demonstrate differences between these six volunteers and the group comprising all other age-matched subjects.

Normative ^{99m}Tc-ECD distribution

Although many normative functional imaging data are available for the assessment of metabolism using ^{18}F-FDG or of perfusion using $H_2{}^{15}O$ PET and ^{99m}Tc-HMPAO, high-resolution, quantitative ^{99m}Tc-ECD perfusion data are very scarce. Apart from smaller series in elderly volunteers [14], only the study of Tanaka et al. [15] has described normal patterns of ECD brain SPET over the whole adult range. Both studies were analysed by visual and/or interactive ROI techniques, without co-registration to individual structural data.

We preferred to include an automated, anatomical standardisation-based VOI analysis alongside the voxel-based SPM method. The former can be seen as an intermediate solution between an operator-dependent, bias-prone and time-consuming ROI analysis, where usually just a fraction of the total brain volume is analysed, and a full voxelwise statistical parametric analysis. One remaining disadvantage of automated VOI analysis lies in the fact that an a priori hypothesis must be made about the localisation and extent

of possible effects, with the consequence that regional effects overlapping these volumes may be missed. However, it was recently shown that if sufficient variance from the VOI measurement is included, the overall performance of a conventional VOI-based analysis can match that of voxel-based analysis for the same clinical discrimination task [16]; this is because the SPM procedure also requires spatial filtering, which degrades the effective resolution. In this study, almost all regions that showed significant gender- or age-related perfusion changes on the SPM analysis also did so on the VOI analysis.

Data in this study are not absolute perfusion data but rather semiquantitative data. Both the VOI and the SPM procedure necessitate normalisation to a reference region or whole brain counts, although comparison of absolute quantitative SPET data is possible [17]. This can be of importance when applied to pathological states, as relative perfusion patterns may no longer apply, and changes in absolute values may impact on pattern interpretation. On the other hand, since physiological and measurement variability in absolute perfusion or metabolism between subjects is much higher (10%–25% [18]) than variability in normalised uptake, discrete changes in relative patterns are easily missed when using only absolute quantitative values.

Hemispheric ^{99m}Tc-ECD uptake asymmetry

^{99m}Tc-ECD uptake was on average 1.4% higher in the right hemisphere for the whole study group. This finding is in quantitative agreement with results reported by other groups [15, 19, 20, 21]. On the other hand, a number of absolute quantitative ^{18}F-FDG PET studies have not found such effects [22, 23]. The predominance of lateral asymmetry in functional imaging studies contrasts with its infrequency in structural age- and gender-related studies.

The timing of the development of cerebral asymmetry and its biological basis are matters of dispute [23]. We found that right-left lateralisation of brain tracer uptake undergoes gender-dependent, age-related changes, especially in the frontotemporal region. Such changes in lateralisation with age have also been reported in previously published perfusion and metabolism studies [20, 24]. Interestingly, we found that while the male human brain undergoes a marked frontal lateralisation with age, the female human brain does not. The biological basis for and neuropsychological consequences of this finding need further research employing appropriate neuropsychological parameters.

rCBF variability

The variation in relative ^{99m}Tc-ECD uptake obtained for each region was as low as 2%–8% and was inversely related to VOI size. In comparison to perfusion data measured with a comparable resolution but with an ROI analysis [14, 15, 19, 25], much lower standard deviations were found; this may be due to both more extensive brain sampling and the objective evaluation of standardised brain regions. Comparable standard deviations have been found using manual ROI techniques; however, these results were obtained in studies with a much lower resolution, which will have decreased regional variance by intrinsic smoothing [21].

Intrasubject variability was substantially smaller than intersubject physiological differences, in agreement with recent HMPAO SPET studies [26, 27, 28]. The interval in this study between scans was relatively long, and the experimental resting conditions were strictly controlled, which is important for optimal reproducibility. As in most other studies, no attempt was made to control for non-specific state-related variables or cognitive activity possibly influencing brain perfusion, which may have contributed to the intra- and intersubject variability. Lower intrasubject reproducibility enables more accurate follow-up studies in the same individual.

The significant correlation between age and variability of VOI measurements is in correspondence with previous literature, and may be attributable to a larger variability of brain atrophy in normal aging, as has been demonstrated by volumetric studies [29].

Age-related changes

Whereas a large amount of both semiquantitative and absolute quantitative data on the effects of aging on brain metabolism and blood flow have been acquired using either PET with ^{18}F-FDG or $H_2{}^{15}O$ or SPET with ^{133}Xe or ^{99m}Tc-labelled ligands ([30 and references therein, 31, 32, 33], such studies have yielded discrepant results in terms of global and regional effects, presumably due to differences in methodology and in screening for their subjects' health status. Nevertheless, most studies indicate that aging does alter the regional cerebral metabolic rate of glucose ($rCMR_{glu}$) and rCBF with a specific frontotemporal pattern, in agreement with our findings. Our findings were insensitive to the non-linear or affine anatomical standardisation (VOI analysis). While in most regions the effect could be best modelled by a linear regression, only in the anterior cingulate cortex was a higher gradient found after the age of 50, this being most prominent in women. We found no arguments for a hockey-stick like aging pattern as described by Mozley et al. [34].

Age-related decreases in rCBF can be associated with changes in attention and short-term memory and in verbal and executive functions. These findings have been taken to indicate a central role for frontal lobe dysfunction and offer neurobiological evidence for a selective age-related decline in frontostriatal system function [32]. Our observation of a lower effect of age on posterior brain tracer uptake represents a more stable or relatively smaller decrease in rCBF in this region than in the rest of the brain. This indicates that the visual and posterior pa-

rieto-occipital association cortices which subserve receptive sensory functions are relatively invulnerable, a finding in line with many neuropsychological studies.

Whether retention of ^{99m}Tc-ECD itself is age-dependent, e.g. via reduction of intracellular enzyme activity, is at present unknown.

Gender-specific differences

The co-variate effects of sexual dimorphism on brain function are more subtle but have also been extensively studied. Neuropsychology, pathology, and structural and functional imaging studies have shown significant effects of gender on cognitive ability, brain disease and non-productive behaviour in areas that subserve speech, visuospatial and memory function [30]. Overall the influence of gender on $rCMR_{glu}$ and rCBF is somewhat controversial, and is probably marginal [22, 30]. However, only a few studies have addressed this issue with reasonable statistical accuracy.

In this study, we found discrete but significantly higher tracer uptake in the cerebellar hemispheres, left anterior temporal cortex and orbitofrontal cortex in men. Women showed a higher tracer uptake bilaterally in the inferior parietal cortex. Such gender-related differences in the parietal tracer uptake are in accordance with the findings of a recent study with ^{99m}Tc-HMPAO by Jones et al. involving 120 adults aged between 50 and 90 years [35]. Recent MRI volumetric studies have shown that there is no gender-related difference in parietal cortex volume in healthy volunteers after correction for global hemisphere differences [36]; this suggests that there are differential functional resting needs in these regions related to visuoconstructional tasks, for which it is known that men show a superior performance.

A relative increase in anterior temporal tracer uptake in men has not been described before, but may tentatively be related to language lateralisation in men and a higher incidence of language-related disturbances after left-sided anterior temporal lesions compared with women [37]. The highly significant lateralisation in frontal tracer uptake which seems to occur preferentially in men is in line with the results obtained with various investigational methods (clinical, electrophysiological, functional imaging), all of which indicate that men may become functionally more lateralised than women.

Methodological considerations

Some authors have demonstrated that cortical atrophy and ventricular enlargement defined on structural imaging do not, on their own, affect the significance of PET measurements of $rCMR_{glu}$ [38]. Others have suggested that after correction for partial volume effects, differences between patients suffering from Alzheimer's disease and controls become non-significant [39]. The most rigid approach to correction for underlying structural changes would be by voxel-based partial volume correction. However, such an approach has not been well validated in clinical situations and therefore we chose not to attempt it at this stage. Studies on detailed correlation with structural data by voxel-based morphometry and correction for partial volume effects are currently underway. In clinical practice, however, a high-resolution 3D MRI dataset may not be available for every individual patient that would allow such correction on a daily basis.

Clinical implications

This study implies that use of ^{99m}Tc-labelled perfusion markers should allow quantitative decision making based on normal ranges for rCBF determined for separate age groups. Of importance is the feasibility of transferring high-resolution SPET databases to other equal- or lower-resolution gamma cameras [40], as this enhances the clinical utility of such anatomically standardised perfusion SPET data for other cameras and departments.

The finding that parietal perfusion was significantly lower in the male group of this dataset indicates that gender-specific normal data would be preferable for the interpretation of rCBF SPET scans in degenerative diseases such as Alzheimer's disease, one of the most accepted indications for brain perfusion SPET in the elderly. Failure to recognise such differences may lead to overinterpretation of SPET studies, with increased false-positive findings in men or false-negative findings in women and evident consequences for individual therapy or studies on preventive or therapeutic drugs.

Conclusion

This study presents a high-resolution normative perfusion database spanning an age range of six decades, based on state-of-the-art imaging methodology and data analysis. Effects of age, gender, asymmetry and their interaction were studied. These effects need to be kept in mind if maximal clinical accuracy is to be attained when using perfusion SPET.

Acknowledgements. This work was supported by a Special Research Grant from Ghent University and the Flemish Government (BOZF 01104699). The authors gratefully acknowledge the logistical support provided by Nuclear Diagnostics Ltd., Sweden and Sun Microsystems, Belgium. We are grateful to Dutoit Medical and Toshiba Europe, in particular I. Verbruggen, for the implementation of transmission hard- and software. We express our gratitude to J.P. Van Haelst for assistance in the preparation of ^{99m}Tc-ECD and to E. Nolf for his aid in the image transfer and conversion. The support of the nursing and technical staff of the University Hospital MRI department in MRI data acquisition and handling is gratefully acknowledged.

References

1. Friston KJ, Ashburner J, Frith CD, Poline JB, Heather JD, Frackowiak RSJ. Spatial registration and normalisation of images. *Hum Brain Mapp* 1995; 2:165–189.
2. Van Laere K, Koole M, Versijpt J, Dierckx R. Non-uniform versus uniform attenuation correction in brain perfusion SPET of healthy volunteers. *Eur J Nucl Med* 2001; 28:90–98.
3. Ebmeier KP, Glabus MF, Prentice N, Ryman A, Goodwin GM. A voxel-based analysis of cerebral perfusion in dementia and depression of old age. *Neuroimage* 1998; 7:199–208.
4. Otte A. The importance of the control group in functional brain imaging [letter]. *Eur J Nucl Med* 2000; 27:1420.
5. Patterson JC, Early TS, Martin A, Walker MZ, Russell JM, Villanueva MH. SPECT image analysis using statistical parametric mapping: comparison of technetium-99m-HMPAO and technetium-99m-ECD. *J Nucl Med* 1997; 38:1721–1725.
6. Hyun Y, Lee JS, Rha JH, Lee IK, Ha CK, Lee DS. Different uptake of ^{99m}Tc-ECD and ^{99m}Tc-HMPAO in the same brains: analysis by statistical parametric mapping. *Eur J Nucl Med* 2001; 28:191–197.
7. Folstein MF, Folstein SE, Mc-Hugh PR. Mini-Mental State: a practical method for grading the cognitive state of patients for the clinician. *J Psychiatr Res* 1975; 12:189–198.
8. Stroop J. Studies of interference in serial verbal reactions. *J Exp Psychol* 1935; 18:643–662.
9. Benton AL, Hamsher K. *Multilingual Aphasia Examination*. Iowa City: AJA Associates, 1989.
10. Wechsler D. *Wechsler Memory Scale – Revised*. New York: Psychological Corporation, 1987.
11. Stuss DT, Stethem LL, Poirier CA. Comparison of three tests of attention and rapid information processing across six age groups. *Clin Neuropsychol* 1987; 1:139–152.
12. Van Laere K, Koole M, Kaupinnen T, Monsieurs M, Bouwens L, Dierckx RA. Non-uniform transmission in brain SPECT using ^{201}Tl, ^{153}Gd and ^{99m}Tc static line sources: anthropomorphic dosimetry studies and differential influence on brain quantification. *J Nucl Med* 2000; 41:2051–2062.
13. Radau PE, Linke R, Slomka PJ, Tatsch K. Optimisation of automated quantification of ^{123}I-IBZM uptake in the striatum applied to parkinsonism. *J Nucl Med* 2000; 41:220–227.
14. Lobaugh NJ, Caldwell CB, Black SE, Leibovitch FS, Swartz RH. Three brain SPECT region-of-interest templates in elderly people: normative values, hemispheric asymmetries, and a comparison of single- and multihead cameras. *J Nucl Med* 2000; 41:45–56.
15. Tanaka F, Vines D, Tsuchida T, Freedman M, Ichise M. Normal patterns on Tc-99m-ECD brain SPECT scans in adults. *J Nucl Med* 2000; 41:1456–1464.
16. Liow JS, Rehm K, Strother SC, et al. Comparison of voxel- and volume-of-interest-based analyses in FDG PET scans of HIV positive and healthy individuals. *J Nucl Med* 2000; 41:612–621.
17. Kogure D, Matsuda H, Ohnishi T, et al. Longitudinal evaluation of early Alzheimer's disease using brain perfusion SPECT. *J Nucl Med* 2000; 41:1155–1162.
18. Maquet P, Dive D, Salmon E, von Frenckel R, Franck G. Reproducibility of cerebral glucose utilization measured by PET and the [^{18}F]-2-fluoro-2-deoxy-D-glucose method in resting, healthy human subjects. *Eur J Nucl Med* 1990; 16:267–273.
19. Krausz Y, Bonne O, Gorfine M, Karger H, Lerer B, Chisin R. Age-related changes in brain perfusion of normal subjects detected by ^{99m}Tc-HMPAO SPECT. *Neuroradiology* 1998; 40:428–434.
20. Markus HS, Ring H, Kouris K, Costa DC. Alterations in regional cerebral blood flow, with increased temporal interhemispheric asymmetries, in the normal elderly: an HMPAO SPECT study. *Nucl Med Commun* 1993; 14:628–633.
21. Catafau AM, Lomena FJ, Pavia J, et al. Regional cerebral blood flow pattern in normal young and aged volunteers: a ^{99m}Tc-HMPAO study. *Eur J Nucl Med* 1996; 23:1329–1337.
22. Gur RC, Mozley LH, Mozley PD, et al. Sex differences in regional glucose metabolism during the resting state. *Science* 1995; 267:528–531.
23. Murphy DG, DeCarli C, McIntosh AR, et al. Sex differences in human brain morphometry and metabolism: an in vivo quantitative magnetic resonance imaging and positron emission tomography study on the effect of aging. *Arch Gen Psychiatry* 1996; 53:585–594.
24. Loessner A, Alavi A, Lewandrowski KU, Mozley D, Souder E, Gur RE. Regional cerebral function determined by FDG-PET in healthy volunteers: normal patterns and changes with age. *J Nucl Med* 1995; 36:1141–1149.
25. Matsuda H, Yagishita A, Tsuji SHK. A quantitative approach to technetium-99m-ethyl cysteinate dimer: a comparison with technetium-99m-hexamethylpropylene amine oxime. *Eur J Nucl Med* 1995; 22:633–637.
26. Deutsch G, Mountz JM, Katholi CR, Liu HG, Harrell LE. Regional stability of cerebral blood flow measured by repeated technetium-99m-HMPAO SPECT: implications for the study of state-dependent change. *J Nucl Med* 1997; 38:6–13.
27. Jonsson C, Pagani M, Ingvar M, et al. Resting state rCBF mapping with single-photon emission tomography and positron emission tomography: magnitude and origin of differences. *Eur J Nucl Med* 1998; 25:157–165.
28. Jonsson C, Pagani M, Johansson L, Thurfjell L, Jacobsson H, Larsson SA. Reproducibility and repeatability of Tc-99(m)-HMPAO rCBF SPET in normal subjects at rest using brain atlas matching. *Nucl Med Commun* 2000; 21:9–18.
29. Blatter DD, Bigler ED, Gale SD, et al. Quantitative volumetric analysis of brain MR: normative database spanning 5 decades of life. *AJNR Am J Neuroradiol* 1995; 16:241–251.
30. Baron JC, Godeau C. Human aging. In: Toga A, Mazziotta JC, eds. *Brain mapping: the systems*. San Diego: Academic Press; 2000:591–604.
31. Goto R, Kawashima R, Ito H, et al. A comparison of Tc-99m HMPAO brain SPECT images of young and aged normal individuals. *Ann Nucl Med* 1998; 12:333–339.
32. Garraux G, Salmon E, Degueldre C, Lemaire C, Laureys S, Franck G. Comparison of impaired subcortico-frontal metabolic networks in normal aging, subcortico-frontal dementia, and cortical frontal dementia. *Neuroimage* 1999; 10:149–162.
33. Schultz SK, O' Leary DS, Ponto LLB, Watkins GL, Hichwa RD, Andreasen NC. Age-related changes in regional cerebral blood flow among young to midlife adults. *Neuroreport* 1999; 10:2493–2496.
34. Mozley PD, Sadek AM, Alavi A, et al. Effects of aging on the cerebral distribution of technetium-99m hexamethylpropylene amine oxime in healthy humans. *Eur J Nucl Med* 1997; 24:754–761.
35. Jones K, Johnson KA, Becker JA, Spiers PA, Albert MS, Holman BL. Use of singular value decomposition to characterize age and gender differences in SPECT cerebral perfusion. *J Nucl Med* 1998; 39:965–973.
36. Coffey CE, Saxton JA, Ratcliff G, Bryan RN, Lucke JF. Relation of education to brain size in normal aging: implications for the reserve hypothesis. *Neurology* 1999; 53:189–196.

37. Davies KG, Bell BD, Bush AJ, Wyler AR. Prediction of verbal memory loss in individuals after anterior temporal lobectomy. *Epilepsia* 1998; 39:820–828.
38. Meltzer CC, Zubieta JK, Brandt J, Tune LE, Mayberg HS, Frost JJ. Regional hypometabolism in Alzheimer's disease as measured by positron emission tomography after correction for effects of partial volume averaging. *Neurology* 1996; 47:454–461.
39. Tanna NK, Kohn MI, Horwich DN, et al. Analysis of brain and cerebrospinal fluid volumes with MR imaging: impact on PET data correction for atrophy. Part II. Aging and Alzheimer dementia. *Radiology* 1991; 178:123–130.
40. Van Laere K, Koole M, Versijpt J, et al. Transfer of normal ^{99m}Tc-ECD brain SPET databases between different gamma cameras. *Eur J Nucl Med* 2001; 28:435–449.
41. Barthel H, Wiener M, Dannenberg C, Bettin S, Sattler B, Knapp WH. Age-specific cerebral perfusion in 4- to 15-year-old children: a high-resolution SPET study using ^{99m}Tc-ECD. *Eur J Nucl Med* 1997; 24:1245–1252.
42. Matsuda H, Tsuji S, Shuke N, Sumiya H, Tonami N, Hisada K. Noninvasive measurement of regional cerebral blood flow using technetium-99m hexamethylpropylene amine oxime. *Eur J Nucl Med* 1993; 20:391–401.
43. Waldemar G, Hasselbalch SG, Andersen AR, et al. ^{99m}Tc-*d,l*-HMPAO and SPECT of the brain in normal aging. *J Cereb Blood Flow Metab* 1991; 11:508–521.
44. Rodriguez G, Warkentin S, Risberg J, Rosadini G. Sex differences in regional cerebral blood flow. *J Cereb Blood Flow Metab* 1988; 8:783–789.
45. Briggs GG, Nebes RD. Patterns of hand preference in a student population. *Cortex* 1975; 11:230–238.